

Ying-Yi Zhang\*, Yun-Gang Li, Xue-Feng Shi and Yuan-Hong Qi

# Effect of Liquid-phase Siliconizing Process on Silicon Diffusion Behavior in Mo Matrix

**Abstract:** MoSi<sub>2</sub> functionally graded coating on Mo substrate is prepared by liquid-phase siliconizing technology. The SEM, GDS and XRD analysis shows that the silicon content in gradient layer appears in three changing regularities. Along the Mo substrate to the surface of the coating, the phase composition of gradient coating changes as follows: Mo → transition layer Mo (main phase) + Mo<sub>3</sub>Si + Mo<sub>5</sub>Si<sub>3</sub> → intermediate layer MoSi<sub>2</sub> → surface layer MoSi<sub>2</sub> (main phase) + Si. According to the Si-Mo diffusion couple and Arrhenius equation, the activation energy ( $Q$ ) was obtained as 430 kJ·mol<sup>-1</sup>, and the Arrhenius dependence of  $D$  on temperature can be described as  $D = 4.9 \times 10^{-3} \exp(-430000/RT) \text{ m}^2/\text{s}$ . The diffusion temperature has an important influence on silicon diffusion coefficient. As the diffusion temperature increases, silicon diffusion coefficient is also gradually increasing.

**Keywords:** liquid-phase siliconizing, Arrhenius, diffusion coefficient, activation energy

**PACS® (2010).** 66.30.-h

\*Corresponding author: Ying-Yi Zhang: State Key Laboratory of Advanced Steel Processes and Products, Central Iron and Steel Research Institute, Beijing 100081, China.  
E-mail: 13716853174@163.com

Yun-Gang Li: College of Metallurgy and Energy, Hebei United University, Tangshan 063009, China

Xue-Feng Shi, Yuan-Hong Qi: State Key Laboratory of Advanced Steel Processes and Products, Central Iron and Steel Research Institute, Beijing 100081, China

nuclear industry, and aerospace fields [3–5]. It is widely used in space reactors emitter, missile exhaust nozzle, satellite rocket boosters, engine blades and high-temperature electrodes and other fields [6, 7]. At present, the main coating preparation methods of molybdenum and its alloys include hot pressed sintering [8], induction plasma deposition [9], electroless deposition [10], chemical vapor deposition (CVD) [11], mechanical alloying [12], and self-propagating high-temperature synthesis (SHS) [13]. When using these methods, however, the MoSi<sub>2</sub> coating surface and cross-section quality is relatively poor and it is very difficult to avoid the pore and crack defects [14–16].

On the other hand, using liquid-phase siliconizing for preparing MoSi<sub>2</sub> coating on Mo matrix has not been reported. This method has many advantages, such as a faster rate of infiltration of silicon, good coating quality, and simple operation process. A large amount of researches has been focused on siliconizing or aluminizing coatings on titanium alloys substrates, and they show that the liquid-phase siliconizing method can remarkably improve the high oxidation resistance of the TiAl-based alloy [17–19]. High silicon content has a marked effect on the growth rate of the layer, and using the melt with a higher silicon content results in formation of the layer with almost a double thickness [20].

In this paper, we propose a new method, using the liquid-phase siliconizing to prepare MoSi<sub>2</sub> functional gradient coating on pure commercial Mo matrix. The effects of siliconizing temperature and time on coating thickness and silicon content distribution are investigated respectively. The silicon diffusion coefficient and the diffusion activation energy are also discussed.

## 1 Introduction

Molybdenum disilicide (MoSi<sub>2</sub>) has attractive properties like high melting point (2303 K = 2030 °C), relatively low density (6.24 g·cm<sup>-3</sup>), excellent resistance to elevated temperature oxidation, and high thermal conductivity (25 W·m<sup>-1</sup>·K<sup>-1</sup>) and electrical resistivity (21.6 × 10<sup>-6</sup> Ω·cm). It is considered to be the most suitable high temperature coating material for the engineering application [1, 2]. MoSi<sub>2</sub> has been rapidly applied in electronics, metallurgy,

## 2 Experimental methods

The polysilicon was used in this work with a purity of 7N. Mo matrices 10 mm × 50 mm were cut from a pure Mo (99.7 wt%) sheet 2 mm thick. The pure polysilicon was melted at 1460–1520 °C by Ar shielding furnace. Then the Mo sample was immersed in the pure polysilicon bath at 1460–1520 °C for 5–20 min (shown in Fig. 1). The phase composition, microstructure and silicon content

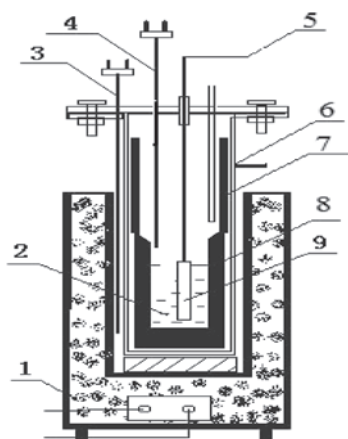


**Fig. 1:** Experimental installation drawing. (1. Electrical furnace; 2. Molten poly-silicon; 3–4. Thermocouple; 5. Molybdenum wire; 6. Alumina tube; 7. Graphite sleeve; 8. Corundum crucible; 9. Mo sheet)

distribution of  $\text{MoSi}_2$  functionally graded coating were investigated by X-ray diffractometer (XRD), scanning electron microscope (SEM) and glow discharge spectrum (GDS). The silicon diffusion in  $\text{MoSi}_2$  functional gradient coating has been studied by diffusion couple experiments at 1460–1520 °C for 5–20 min. The silicon diffusion coefficient and the diffusion activation energy are also calculated by Arrhenius equation [21].

### 3 Results and discussion

#### 3.1 Microstructure and growth of the gradient coatings

The  $\text{MoSi}_2$  functional gradient coatings on pure commercial Mo matrix have been obtained by liquid-phase sili-

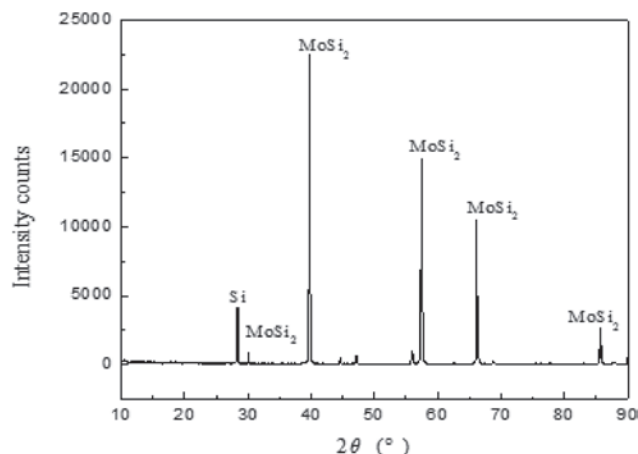


**Fig. 2:** XRD patterns of  $\text{MoSi}_2$  functional gradient coating surface

conizing method. According to the XRD analysis results (Fig. 2), the surface of  $\text{MoSi}_2$  functionally graded coating is mainly constituted by Si and  $\text{MoSi}_2$ . Fig. 3 shows the surface and cross-sectional SEM images of the  $\text{MoSi}_2$  functionally graded coating prepared at 1500 °C for 20 minutes. The SEM analysis shows that, along the Mo substrate to the surface of the coating, the phase composition of gradient coating changes as follows: Mo → transition layer Mo (main phase) +  $\text{Mo}_3\text{Si}$  +  $\text{Mo}_5\text{Si}_3$  → intermediate layer  $\text{MoSi}_2$  → surface layer  $\text{MoSi}_2$  (main phase) + Si [22].

The effect of the siliconizing conditions on the Si concentration distribution is presented in Fig. 4. The silicon content in gradient layer appears in three changing regularities. At the surface of the coating, the coating phase structure is composed by Si and  $\text{MoSi}_2$ , so the silicon content is highest (> 65 mass%). This is caused by the surface composite structure of  $\text{MoSi}_2$  and Si. At the intermediate layer, the silicon basic content remains unchanged (30 to 35 wt%). Si to Mo ratio is 2:1, which meets the generation conditions of  $\text{MoSi}_2$ . At the transi-

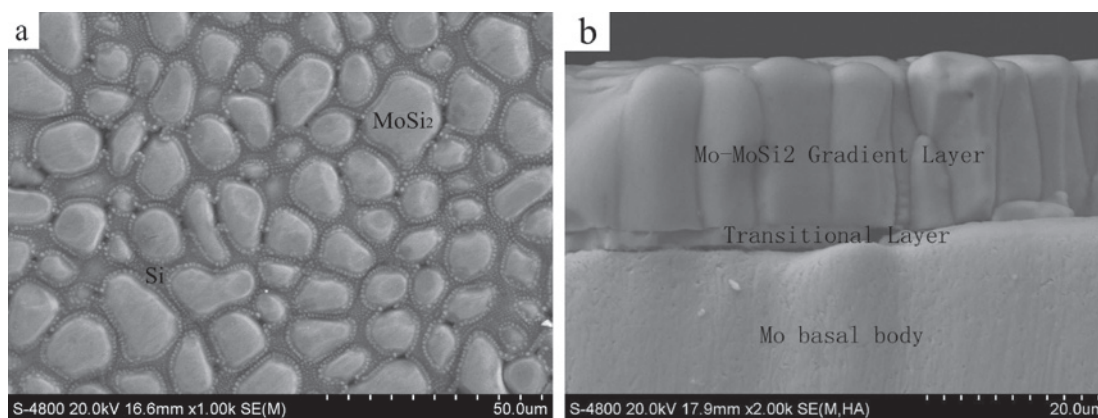


**Fig. 3:** SEM photos of coating surface (a) and cross-section (b)

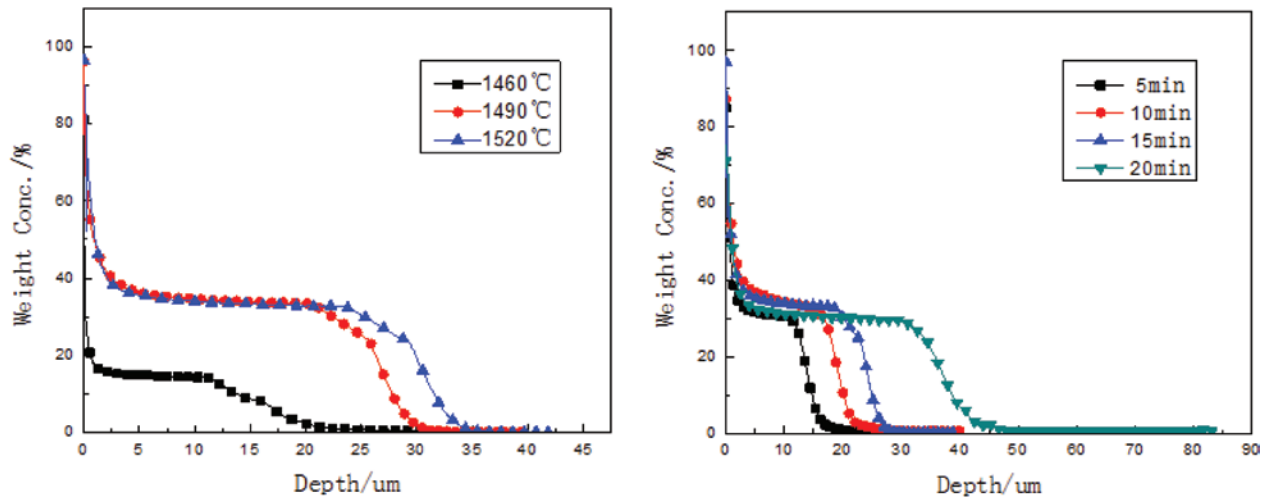


Fig. 4: Effect of the siliconizing conditions on the Si concentration distribution

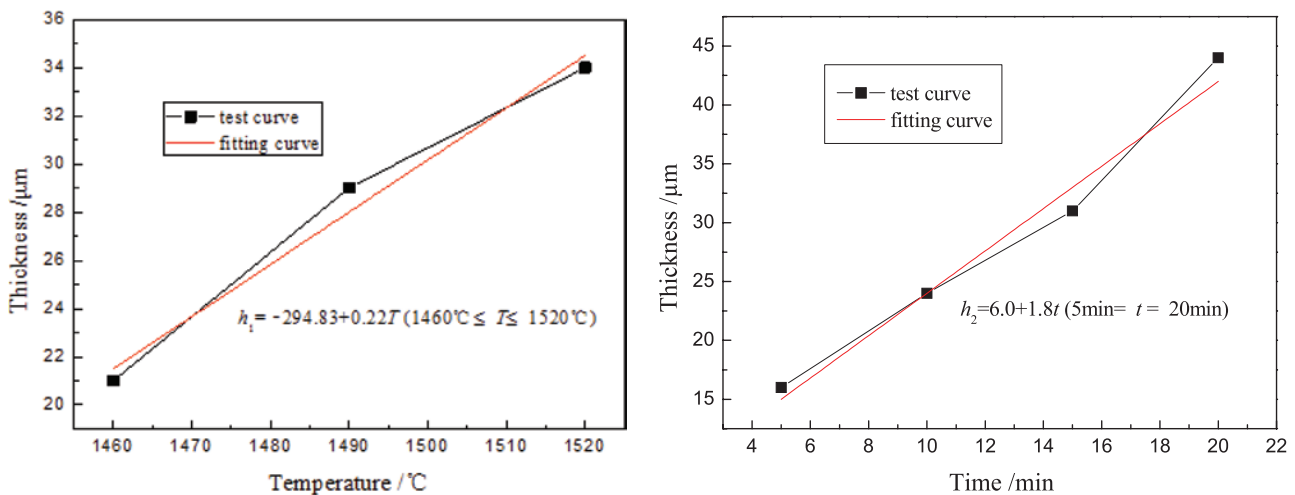


Fig. 5: Effect of the siliconizing conditions on the coating thickness

tional layer, the coating phase structure is composed by  $\text{Mo}_3\text{Si}$ ,  $\text{Mo}_5\text{Si}_3$  and Mo (main phase), so the silicon content is lowest. It was found that the thickness of the  $\text{MoSi}_2$  functional gradient coatings increased with increase in siliconizing temperature ( $T$ ) and siliconizing time ( $t$ ) (shown in Fig. 5). The increase of the thickness of the  $\text{MoSi}_2$  functional gradient coatings can be described as:  $h_1 = -294.83 + 0.22T$  ( $1460^\circ\text{C} \leq T \leq 1520^\circ\text{C}$ ),  $h_2 = 6.0 + 1.8t$  ( $5 \leq t \leq 20$  min), in which  $h_1$  and  $h_2$  are the coating thickness.

### 3.2 Diffusion equation of silicon

In the liquid-phase siliconizing process, silicon concentration changes along with the diffusion time, so this dif-

fusion belongs to the unsteady diffusion. For simplicity, assume that the diffusion coefficient  $D$  is constant, and the Fick's second law is as follows:

$$\frac{\partial c}{\partial t} = D \frac{\partial^2 c}{\partial x^2} \quad (1)$$

where  $c$  is the concentration of diffusion components ( $\text{g}/\text{cm}^3$ ),  $D$  is diffusion coefficient ( $\text{cm}^2/\text{s}$ ), and  $x$  is diffusion depth. After the siliconizing, the polysilicon solution adhesion on the surface grain boundary resulted in an increase in surface silicon content. So the silicon of surface grain boundary was not involved in diffusion and phase transformation reaction, the siliconizing process in accordance with the diffusion couple model, the silicon solid state diffusion forms a diffusion couple (Fig. 6). Therefore the initial conditions and boundary condition

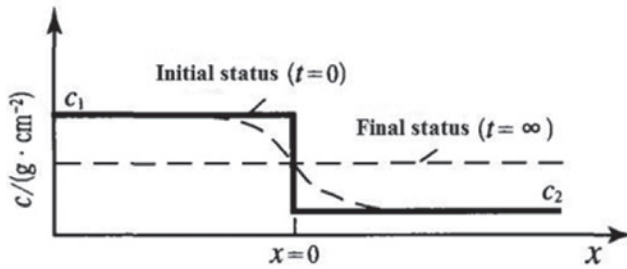


Fig. 6: The silicon concentration distribution of Si-Mo diffusion couple. (This silicon concentration ( $c_1$ ) has not included the silicon concentration of surface grain boundary.)

can be assumed as follows: ①  $t = 0$ ,  $x > 0$ ,  $C = C_2$ ; ②  $x < 0$ ,  $C = C_1$ ; ③  $x = 0$ ,  $C_1 = C_0 = 100\%$ ; ④  $x = +\infty$ ,  $C = C_2 = 0$ .

Because the silicon diffusion in the Mo matrix accord with one dimensional semi-infinite diffusion model, using the error function method to solve the Eq. (1) and get a solution of Grube equation [23].

$$c(x, t) = (c_2 + c_1) + (c_2 - c_1) \cdot \frac{2}{\sqrt{\pi}} \int_0^\beta e^{-\beta^2} d\beta \quad (2)$$

where the  $2/\sqrt{\pi} \int_0^\beta e^{-\beta^2} d\beta$  is called the error function  $\text{erf}(\beta)$ , ( $\text{erf}(\beta) = 2/\sqrt{\pi} \int_0^\beta e^{-\beta^2} d\beta$ ). So Eq. (2) can be rewritten as follows:

$$c(x, t) = (c_2 + c_1) + (c_2 - c_1) \cdot \text{erf}\left(\frac{x}{2\sqrt{Dt}}\right) \quad (3)$$

Take the boundary conditions into Eq. (4) obtained the diffusion equation of silicon in the Mo matrix.

$$c(x, t) = 1 - \text{erf}\left(\frac{x}{2\sqrt{Dt}}\right) \quad (4)$$

where  $c(x, t)$  is the silicon concentration (mass%),  $D$  is diffusion coefficient ( $\text{cm}^2/\text{s}$ ),  $x$  is diffusion depth ( $\mu\text{m}$ ).

### 3.3 Effect of siliconing conditions on silicon diffusion

Temperature has a significant influence on the diffusion coefficient [24]. Typically, an Arrhenius dependence of  $D$  on temperature is assumed [25].

$$D = D_0 \exp\left(-\frac{Q}{RT}\right) \quad (5)$$

$$\ln D = \ln D_0 - \frac{Q}{RT} \quad (6)$$

where  $D$  is the temperature-dependent atomic diffusivity. The pre-exponential factor,  $D_0 (\text{m}^2 \cdot \text{s}^{-1})$ , and activation energy,  $E (\text{J} \cdot \text{mol}^{-1})$ . As can be seen, the diffusion coefficient with the temperature rising exponentially increases. This is due to the high temperature making the ion number and vacancy concentration meeting the transition energy conditions significantly increase. So, with the increase of siliconizing temperature, the diffusion coefficient of silicon is also gradually increasing, the diffusion reaction becomes more easily. On the crystal surface and grain boundaries, the atoms are arranged irregularly which is different with the internal arrangement of atoms. So the atoms of crystal surface and grain boundaries have higher energy states and their diffusion activation energy is smaller. Therefore, the atoms of crystal surface and grain boundary diffuse faster and the coating surface has high silicon content in the siliconizing process. In addition, the atoms diffusion activation energy is also affected by the nature of atoms, such as atomic size, and other affinity element size and other factors [26]. When the atomic sizes are close, the lattice distortion and diffusion activation energy are smaller, and the atomic diffusion coefficient is bigger. Due to the atomic radius of Si and Mo being similar ( $r_{\text{Si}} = 1.34 \text{ nm} \sim 1.17 \text{ nm}$ ,  $r_{\text{Mo}} = 1.39 \text{ nm}$ ), electronegativity is also close ( $X_{\text{Si}} = 1.80 \sim 1.90$ ,  $X_{\text{Mo}} = 1.80 \sim 2.10$ ) [27]. So the diffusion activation energy of Si and Mo atoms is smaller and atomic diffusion is easier.

All the penetration profiles ( $C_{\text{Si}}(x, t)$  against  $x$ ) are displayed in Fig. 4. Put the  $C_{\text{Si}}(x, t)$  and diffusion depth ( $x$ ) into Eq. (4) and combine error function table of  $\text{erf}(\beta)$  to calculate the diffusion coefficient under different siliconizing temperatures and times. Get a desired estimate of  $D$  as a function of time or alternatively as a function of temperature (shown in Fig. 7). With fixed diffusion temperature, diffusion time has no effect on silicon diffusion coefficient, but has an important influence on the thickness of the gradient coating. With fixed diffusion time, diffusion temperature has an important influence on silicon diffusion coefficient. When the diffusion temperature increases, the ion number and vacancy number rapidly increase to meet the transition energy condition. The silicon diffusion coefficient is also gradually increasing, and the silicon diffusion activation energy is smaller in molybdenum substrate. The diffusion mechanism of Si, Mo atoms belongs to the transposition diffusion mechanism, and diffusion temperature is the main factor on the diffusion rate of silicon.

The corresponding Arrhenius plots is shown in Fig. 8, where  $\ln D_{\text{Si}}$  is the ordinate axis and  $1/T$  is the abscissa. A departure from the Arrhenius law is observed, as expected. The results can be fitted by

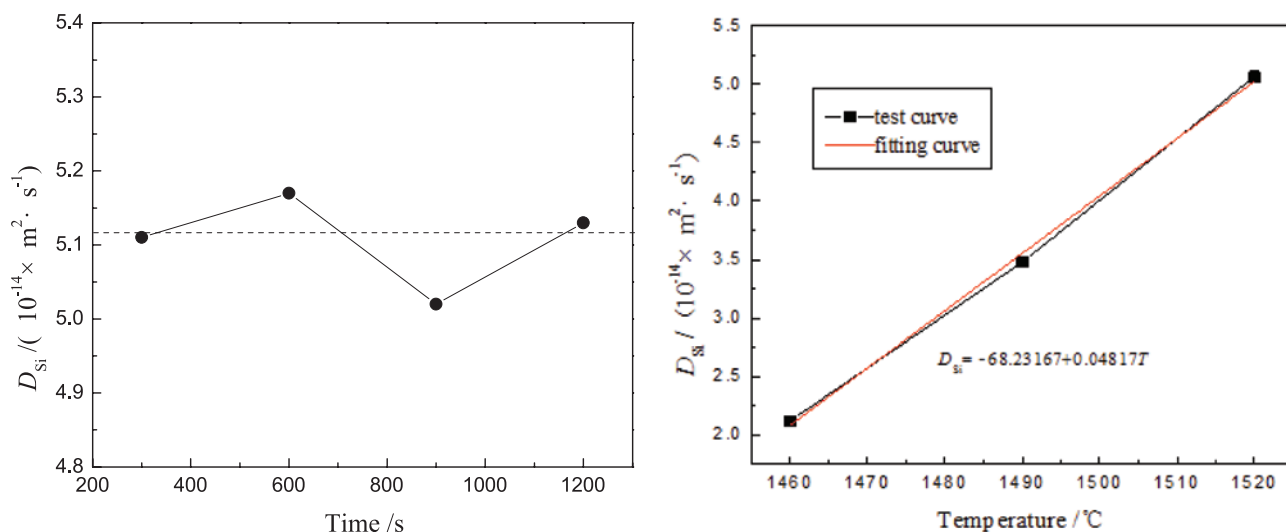


Fig. 7: Effect of siliconizing conditions on silicon diffusion coefficient

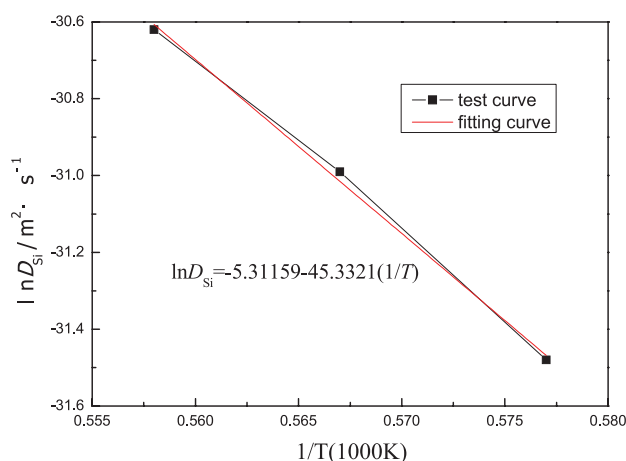


Fig. 8: Arrhenius plots for Si diffusion in Mo matrix

$$\ln D_{\text{Si}} = -5.31159 - 45.3221 (1/T) \quad (R^2 = 0.9996) \quad (7)$$

Substituting Eq. (7) into Eq. (6), we obtained the parameters  $D_0$  and  $Q$ . The estimated diffusion frequency factor ( $D_0$ ) was about  $4.9 \times 10^{-3} \text{ m}^2/\text{s}$ , and the diffusion activation energy ( $Q$ ) was about  $430 \text{ kJ}\cdot\text{mol}^{-1}$ .

## 4 Conclusions

The  $\text{MoSi}_2$  functional gradient coatings on pure commercial Mo matrix have been obtained by liquid-phase siliconizing method. The thickness of the  $\text{MoSi}_2$  functional gradient coatings increased with increase in siliconizing temperature ( $T$ ) and siliconizing time ( $t$ ). It can be described as:  $h_1 = 6.0 + 1.8t$  ( $5 < t < 20 \text{ min}$ ),  $h_2 =$

$-294.83 + 2.2T$  ( $1460^\circ\text{C} < T < 1520^\circ\text{C}$ ). According to the diffusion equation of silicon in the Mo matrix ( $c(x,t) = 1 - \text{erf}(x / 2\sqrt{Dt})$ ), the diffusion coefficient of the Si-Mo system was obtained. The diffusion time has a little influence on silicon diffusion coefficient, but has an important influence on the thickness of the gradient coating. The diffusion temperature has an important influence on silicon diffusion coefficient. When the diffusion temperature increases, silicon diffusion coefficient is also gradually increasing. According to the Arrhenius equation, the activation energy ( $Q$ ) was obtained as  $430 \text{ kJ}\cdot\text{mol}^{-1}$ , and the Arrhenius dependence of  $D$  on temperature can be described as  $D = 4.9 \times 10^{-3} \exp(-430000/RT) \text{ m}^2/\text{s}$ .

**Acknowledgments:** The authors wish to acknowledge Dr. Y.-G. Li and J. Zhao for their collaboration in this work.

This work was partially supported by the National Natural Science Foundation of China (50474079) and Hebei Natural Science Foundation of China (E2010000945).

Received: September 18, 2013. Accepted: November 10, 2013.

## References

- [1] T.A. Kircher and E.L. Courtright. *Materials Science and Engineering A*, 1992, A 155(1/2): 67–74.
- [2] P.Z. Feng, X.H. Qu, Akhtar Farid and S.H. Islam. *Rare Metals*, 2006, 25(3): 225.
- [3] R. Rapp, *Materials for extreme environments*, Mater., 2006, 9(5): 6–8.
- [4] John H. Perepezko. *Science*, 2009, 20: 1068.

- [5] S. Tang, J. Deng, S. Wang, W. Liu and K. Yang. *Mater. Sci. Eng., A*, 2007, 465: 1–7.
- [6] R.H. Zee, Z. Xiao, B.A. Chin and J. Liu. *Journal of Materials Processing Technology*, 2001, 113: 75.
- [7] J.H. Yan, H.M. Xu, H.A. Zhang, et al. *Rare Metals*, 2009, 28(4): 418–422.
- [8] H.M. Zhou, J. Li and D.Q. Yi. *ISRN Materials Science*, 2012, 5042(10): 1–8.
- [9] X.B. Fan and Takamasa Ishigaki. *J. Am. Ceram. Soc.*, 1999, 82(8): 1965–1968.
- [10] M. Shoeib and M.A. Maamoun. *Tribotest Journal*, 2002, 9(1): 49–56.
- [12] J.H. Yan, Y.L. Li and H.A. Zhang. *J. Cent. South Univ. Technol.*, 2008, 15: 301–304.
- [13] P.Z. Feng, W.S. Liu, S.H. Islam, et al. *Powder Metallurgy*, 2011, 54(1): 79–83.
- [14] L. Yin, L. Yang and D. Yi. *Materials Science and Technology*, 2005, 21(5): 579–582.
- [15] V.A. Gorshkov, V.I. Yukhvid, N.T. Andrianov and E.S. Lukin. *Neorganicheskie Materialy.*, 2009, 45(5): 560–564.
- [16] Q.-G. Fu, H.-J. Li, K.-Z. Li and X.-H. Shi. *Surface Engineering*, 2008, 24(5): 383–387.
- [17] M. Goral, L. Swadzba, G. Moskal, et al. *Intermetallics*, 2009, 17: 965–967.
- [18] H.P. Xiong, Y.H. Xie, W. Mao, et al. *Scripta Materialia*. 2003, 49: 1117–1122.
- [19] S.H. Chen, L.Q. Li and Y.B. Chen. *Trans. Nonferrous Met. Soc.*, 2010, 20: 64–70.
- [20] T. Kubatík, M. Jáglová, E. Kalabisová and V. Cíhal. *Journal of Alloys and Compounds*, 2011, 509: 5493–5499.
- [21] Z.S. Ren, X.J. Hu, X.X. Xue, et al. *Journal of Alloys and Compounds*, 2013, 580(15): 182–186.
- [22] Ying-Yi Zhang, Yun-Gang Li, Yong-Hong Qi, Xue-Feng Shi. *Rare Metals*, 2013 (in press).
- [23] R.Z. Yang, D.H. Yu and J. Zhao. *Journal of Tongji University (Natural Science)*, 2004, 32(9): 1145–1148.
- [24] Z.F. Wei. Solid-state diffusion and phase transformation of metals. Mechanical Industry Press., Beijing, 1998.
- [25] Z. Li, X.P. Su, Y.H. He, et al. *The Chinese Journal of Nonferrous Metals*, 2008, 18(9): 1639–1644.
- [26] Donald R. Askeland. The Science and Engineering of Materials. Boston: PWS-Kent Publishing, 1989, p. 121.
- [27] Tatsuo Tabaru, Kazuhisa Shobu, Michiru Sakamoto, et al. *Intermetallics*, 2004, 12: 33–41.